scientific reports

Check for updates

OPEN

Mechanistic and comparative laboratory assessment of lime dosage and uniaxial geogrid on the strength and durability of classified lateritic subgrade

Udeme Udo Imoh[1], Akindele Christopher Apata[2], Abdulazeez Muritala Bolorunduro[2] & Majid Movahedi Rad[1]✉

This study presents a mechanistic and comparative laboratory assessment of lime stabilization and uniaxial geogrid reinforcement, applied independently and in combination, to improve the engineering performance of a classified A-7-6 (CL–ML) lateritic subgrade from Ogun State, Nigeria. The objective was to evaluate the effect of lime dosage and geogrid inclusion on the short- and long-term California Bearing Ratio (CBR), Unconfined Compressive Strength (UCS), and Resilient Modulus (MR), and to test the hypothesis that chemical and mechanical stabilization mechanisms act synergistically to enhance stiffness and durability. Quicklime (CaO > 90%) was added at 2–8% by dry weight, while the geogrid used was uniaxial polypropylene with an aperture size of 30 mm and tensile strength of 22 kN/m. Specimens were prepared by mixing, compacting, and curing at 25 ± 2 °C and 95 ± 2% RH for 7, 14, and 28 days, then tested according to ASTM and AASHTO standards. Each condition was replicated thrice, and the data were analyzed using one-way ANOVA ($p < 0.05$). Results showed that lime treatment reduced the plasticity index from 30 ± 1.2 to 6 ± 0.5%, increased UCS from 300 ± 15 to 950 ± 40 kPa and improved soaked CBR from 23 ± 1.1 to 57.5 ± 2.3% after 28 days. Single and double geogrid layers enhanced soaked CBR to 33 ± 1.4% and 43 ± 1.7%, respectively, with negligible strength loss after three moisture cycles, confirming durability under wetting–drying conditions. Combined lime–geogrid stabilization achieved the highest performance, with CBR > 65%, MR > 90 MPa, and UCS > 1.0 MPa, exceeding AASHTO subgrade requirements. The findings demonstrate that lime primarily enhances chemical bonding, whereas geogrid reinforcement improves mechanical confinement; their combination offers a durable, cost-effective, and low-carbon alternative to conventional cement stabilization for tropical lateritic subgrades.

Keywords Lateritic soil, Lime stabilization, Geogrid reinforcement, California bearing ratio, Unconfined compressive strength, Pavement subgrade

Abbreviations

AASHTO	American Association of State Highway and Transportation Officials
ASTM	American Society for Testing and Materials
BS	British Standard
CBR	California bearing ratio
CL–ML	Low-plasticity clay–silt (unified soil classification system)
CaO	Quicklime (calcium oxide)
$Ca(OH)_2$	Hydrated lime (calcium hydroxide)
LL	Liquid limit
PL	Plastic limit
PI	Plasticity index

[1]Department of Structural and Geotechnical Engineering, Faculty of Architecture, Civil Engineering and Transport Sciences, Széchenyi István University, Győr 9026, Hungary. [2]Department of Civil Engineering, University of Lagos, Lagos, Nigeria. ✉email: majidmr@sze.hu

MDD	Maximum dry density
OMC	Optimum moisture content
NMC	Natural moisture content
UCS	Unconfined compressive strength
XRD	X-ray diffraction
XRF	X-ray fluorescence
TEM	Transmission electron microscopy
SEM	Scanning electron microscopy
USCS	Unified soil classification system
PP	Polypropylene (geogrid material)
SWCC	Soil–water characteristic curve
RM	Resilient modulus
C&D	Construction and demolition (waste)
R^2	Coefficient of determination
w/c	Water-to-cement ratio (if mentioned)

The performance and longevity of pavement structures fundamentally depend on the mechanical behavior of subgrade soils. In tropical regions such as southwestern Nigeria, subgrades often consist of highly weathered lateritic soils with variable mineralogy and high plasticity, which significantly reduce bearing capacity and deformation resistance[1,2]. Field investigations at the present study site in Ogun State, Nigeria, revealed a lateritic soil classified as A-7-6 under the AASHTO system and CL–ML under the USCS. The soil exhibited a liquid limit of 58%, a plasticity index of 30%, a soaked CBR of 22%, and a natural moisture content of 15%. X-ray fluorescence (XRF) confirmed a predominantly siliceous–aluminous composition (SiO_2 =52%, Al_2O_3 =25%) with minor ferric and calcium oxides. These properties, that is, high plasticity, low strength, and moisture susceptibility, are typical of problematic laterites that deform excessively under traffic and wet season conditions, leading to premature pavement distress such as rutting, cracking, and shear failure[3,4].

The stabilization of such soil is an established strategy for improving the workability, strength, and stiffness. Among the chemical stabilizers, lime remains one of the most effective for clayey and lateritic soils, promoting improvements through cation exchange, flocculation–agglomeration, and pozzolanic reactions that produce calcium silicate and aluminate hydrates[5–7]. Typical lime dosages of 4–8% by dry soil weight improve plasticity, compaction, and long-term strength. Conversely, geogrid reinforcement enhances the subgrade performance by providing tensile restraint and mechanical interlocking with soil aggregates, redistributing applied stresses, and limiting lateral deformation[8,9]. Uniaxial polypropylene geogrids with aperture sizes of 25–40 mm and tensile strengths exceeding 20 kN/m have shown significant benefits in reducing permanent strain and improving the resilient modulus in both cohesive and granular soils[10,11]. Despite their proven effectiveness, comparative evidence under identical laboratory conditions remains scarce, particularly for lateritic soils.

Recent studies have emphasized the potential of sustainable hybrid stabilizers. Phummiphan et al.[12] demonstrated that high-calcium fly ash-based geopolymers markedly improved the unconfined compressive strength (UCS) and durability of marginal lateritic soils, with curing duration strongly influencing strength gain. Nano-geopolymer treatments further enhance stiffness and moisture durability, achieving significant increases in the resilient modulus and reduced crack susceptibility in expansive and tropical soils[13,14]. Incorporating industrial and agricultural wastes, such as limestone powder, rock powder, and palm-bunch ash, has produced comparable stabilization performance to cement, while reducing embodied carbon[15]. Mechanistic studies have shown that lime–soil interactions form denser matrices and reduce pore connectivity, thereby improving long-term resistance to moisture-induced degradation[7,16,17].

Parallel advances in geosynthetics have demonstrated the efficacy of geogrid reinforcement in enhancing the bearing capacity and minimizing the rut depth under cyclic loading[18,19]. Geogrids act as confinement elements, mobilizing tensile forces that improve the load transfer and stiffness, particularly in weak subgrades subjected to repeated traffic loads[20]. Combined lime–geogrid systems have recently shown synergistic effects, where chemical bonding enhances cohesion and mechanical interlocking improves deformation resistance[21,22]. Nevertheless, the published data remains largely qualitative, and few studies have quantitatively linked the chemical composition, microstructure, and mechanical response under unified testing frameworks.

Further research has applied artificial intelligence and machine learning (ML) to predict the stiffness, CBR, and swelling pressure in stabilized soils[21,23,24]. However, these predictive models require extensive, high-quality experimental datasets for calibration, which are limited to lateritic soils treated with lime and geogrids. Moreover, long-term durability under moisture cycles, constructability, and life-cycle sustainability have not been systematically evaluated, leaving a knowledge gap in mechanistic design and practical implementation[25,26]. From this review and synthesis of prior studies (Table 1), three major gaps were identified: (1) lack of side-by-side laboratory comparisons between lime stabilization and geogrid reinforcement on a single lateritic soil under standardized compaction and curing conditions; (2) insufficient mechanistic linkage between chemical composition, microstructure, and micromechanical response (UCS, CBR, and resilient modulus); and (3) limited evaluation of long-term durability, environmental impact, and cost efficiency relative to cement-based stabilization. These gaps hinder the rational selection and optimization of stabilization techniques for tropical lateritic soils.

This study addresses these gaps through a mechanistic and comparative laboratory assessment of lime stabilization and uniaxial geogrid reinforcement applied to A-7-6 lateritic soil from Ogun State, Nigeria. This study systematically evaluated the short- and long-term effects of lime dosage (2–8% by dry weight) and geogrid configuration on California Bearing Ratio (CBR), unconfined compressive strength (UCS), resilient modulus, and durability under soaked and unsoaked conditions. Microstructural analyses using X-ray fluorescence (XRF),

X-ray diffraction (XRD), and transmission electron microscopy (TEM) were performed to elucidate the chemical and physical mechanisms governing the improvement of performance. The central hypothesis is that lime primarily enhances strength through pozzolanic bonding, whereas geogrid reinforcement improves stiffness and deformation control through mechanical interlocking, and that a combined lime–geogrid system yields superior overall performance compared with either method alone. The novelty of this work lies in its unified mechanistic comparison of chemical and mechanical stabilization strategies using identical lateritic soil, test conditions, and evaluation metrics. By integrating compositional, microstructural, and mechanical data, this study develops a holistic understanding of stabilization mechanisms, identifies optimal treatment parameters, and proposes a sustainable, lower-carbon alternative to cement-based subgrade stabilization for tropical highway infrastructure. These findings are expected to support mechanistic empirical pavement design frameworks and contribute to the broader adoption of environmentally responsible ground improvement techniques in developing regions.

Objectives of the study

Here are clear, study-aligned objectives:

- The chemical and mineral composition of the soil and lime were determined using XRF/XRD to assess the reactivity for pozzolanic stabilization.
- Quantify the Effects of lime content (2–8% by dry soil weight) on compaction behavior (MDD, OMC), plasticity (LL, PL, PI), strength (UCS), and bearing capacity (CBR—soaked/unsoaked).
- The geogrid reinforcement performance (uniaxial PP; single vs. double layer, varying embedment depths) on soaked/unsoaked CBR and UCS of compacted soil was evaluated.
- Compare by side the effectiveness of lime stabilization versus geogrid reinforcement under identical laboratory conditions.
- Optimal lime dosage (mechanical/strength optimum) and effective geogrid configuration for lateritic subgrade improvement.
- Investigate microstructural mechanisms via TEM (and link to macro-properties) to explain strength/stiffness gains with lime and geogrid.
- Assess the potential benefits of a combined strategy (lime + geogrid) for heavily trafficked moisture-susceptible pavements.

Significance of this study

This study is significant in several respects, both for geotechnical research and practical highway engineering applications.

- Addressing Weak Subgrades in the Tropics: Lateritic soils dominate much of West Africa, yet their high plasticity and low shear strength often lead to premature pavement failure. By improving their performance, this study directly addresses one of the root causes of Nigeria's road deterioration.
- Comparative Insight into Two Widely Used Techniques: Although lime stabilization and geogrid reinforcement are well established, side-by-side evaluations under identical conditions are limited. This study provides a direct comparison, clarifying where each method excels (lime for chemical strength gain and geogrid for stiffness and deformation resistance).
- Development of Optimal Stabilization Strategies: This study identifies the optimum lime content (~6%) and effective geogrid configurations (single vs. double layer), providing engineers practical benchmarks for field applications rather than relying solely on generic recommendations.
- Integration of Microstructural and Mechanical Analysis: By linking TEM and XRF/XRD findings to macro-scale strength and compaction behavior, this study provides a mechanistic understanding of how stabilization works, bridging material science and engineering performance.

No.	Authors	Materials	Key findings	Limitation/gap
1	Cabalar et al.[27]	Silt with waste limestone powder	Improved strength and compressibility using quarry fines	Durability and field-scale testing lacking
2	Cabalar et al.[28]	Organic soil plus rock powder	Increased UCS; reduced compressibility	Limited microstructural analysis
3	Mohajerani et al.[29]	Recycled rubber inclusions	Enhanced ductility; promoted circular economy	Lack of design standardization
4	Phummiphan et al.[12]	Clay with metal waste	Significant strength gain; good subgrade potential	Only single soil type evaluated
5	Phummiphan et al.[12]	Lateritic soil plus fly ash geopolymer	Curing time strongly affects UCS	Long-term durability untested
6	Al-Taie et al.[30]	Lime-treated expansive clay	Reduced swelling, improved strength	SWCC–strength coupling unassessed
7	Mohammadinia et al.[31]	Recycled C&D plus lime	Improved stiffness and bonding	Environmental impact is not quantified
8	Ikechukwu et al.[13]	Nano-geopolymer plus expansive soil	Increased resilient modules, reduced cracks	Durability and moisture cycles were not tested
9	Onyelowe et al.[32]	AI model for geopolymer-treated soil	Reliable prediction of stiffness gains	Requires experimental validation
10	Patel et al.[33]	Lime-treated laterite	Strength improved; cost-effective vs. cement	No geogrid comparison
11	Amare et al.[34]	Laterite with hybrid binders	Combined mechanical/chemical treatment effective	Lack of long-term durability data
12	Styer et al.[10]	Geogrid-reinforced subgrades	Reduced rutting under cyclic load	No comparison with chemical methods

Table 1. Summary of recent studies on soil stabilization and reinforcement of lateritic and fine-grained soils.

- Contribution to Sustainable Infrastructure: The findings suggest that combining lime and geogrid can reduce reliance on cement-based stabilization, lowering the carbon footprint and construction costs while enhancing pavement service life.
- Practical Application for Policy and Practice: Results can inform highway agencies, contractors, and policy-makers in developing regions of cost-effective and durable methods for upgrading subgrade soils, supporting better road performance, reduced maintenance, and improved transport reliability.

Materials and methods

A comprehensive experimental program was undertaken to achieve a thorough characterization of the tested materials in accordance with established international standards. Geotechnical investigations include sieve analysis, determination of Atterberg limits, measurement of natural moisture content, specific gravity determination, standard compaction testing, California Bearing Ratio (CBR) testing, and unconfined compressive strength (UCS) testing. These tests provide fundamental engineering properties of soils and aggregates and offer insights into their classification, strength, and suitability for engineering applications. In addition to conventional laboratory characterization, advanced analytical techniques have been employed to obtain a more comprehensive understanding of materials at the microstructural and compositional levels. Transmission Electron Microscopy (TEM) was used to investigate the surface morphology, microstructural features, and localized chemical composition with high spatial resolution, enabling the identification of fine-scale structural characteristics. X-ray Fluorescence (XRF) analysis complemented this by providing quantitative mineralogical and chemical composition data for soils, rocks, and slag-based aggregates. XRF is particularly effective for the characterization of fine-grained soils, where its high accuracy and reliability in determining the crystalline phases and elemental composition make it an essential tool for geotechnical and material research. Figure 1 shows the materials used in the experiments.

Materials

Lateritic soil

Lateritic soils are highly weathered tropical soils characterized by significant concentrations of iron and aluminum oxides resulting from prolonged chemical weathering in hot and humid environments[33–43]. These soils are widely encountered in engineering projects across West Africa and are often used as subgrade or fill materials in road construction. Their variable mineralogy, particle size distribution, and plasticity necessitate rigorous sampling and preparation protocols to obtain representative results. In this study, lateritic soil was collected from a road construction site in Ogun State, Nigeria (Fig. 2), at a depth of 1.0–1.5 m. Sampling below the topsoil horizon was intentional to minimize the influence of organic matter, root structures, and surface contaminants, which can significantly alter geotechnical properties[35]. The choice of site was guided by the representativeness of the typical subgrade conditions in the region. Samples were sealed in polythene bags immediately after collection to preserve in situ moisture conditions and transported to the laboratory in accordance with the BS 1377 (1990) standards for soil testing[44,45]. Upon arrival, the samples were stored in a controlled dry environment and air-dried for 72 h to remove residual moisture, thereby preventing microbial activity and facilitating particle size reduction without altering soil mineralogy. Manual crushing with a rubber mallet was employed to disaggregate soil clods while avoiding excessive particle breakdown, which is a critical step in preserving the natural gradation ASTM D421[46]. The material was first sieved through a BS No. 4 (4.25 mm) sieve, followed by a 2.0 mm (No. 10) sieve, ensuring the removal of oversized particles for uniformity in laboratory tests. Homogenization via the quartering method further minimized variability, ensuring a representative sample for subsequent characterization tests such as Atterberg limits, compaction, and shear strength analyses.

This systematic procedure reflects internationally recognized practices and ensures reproducibility, which is a crucial factor in geotechnical investigations. Appropriate sample preparation mitigates the risk of experimental errors and supports the reliability of the data used in pavement design, foundation assessment, and material classification frameworks, particularly for tropical soils that often exhibit high heterogeneity.

(a) laterite (b) Geogrid reinforcement (c) lime

Fig. 1. Materials for experimental analysis. **a** Laterite; **b** geogrid reinforcement; **c** lime.

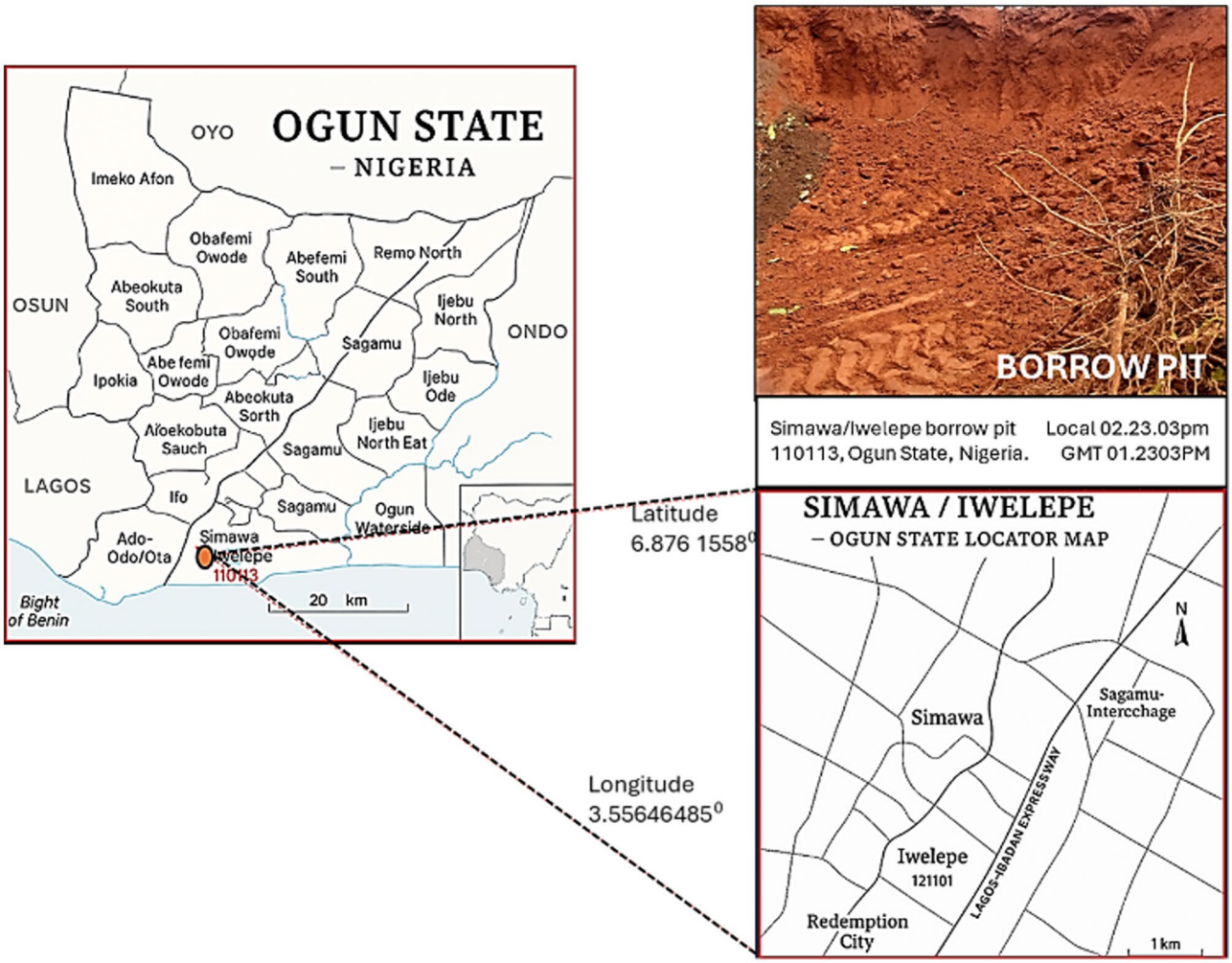

Fig. 2. Map of sampling site at Ogun State and borrow pit location.

Lime

Commercial hydrated lime [Ca $(OH)_2$] was procured locally in 25 kg bags and stored in airtight containers to minimize exposure to atmospheric CO_2 and moisture, thereby preventing carbonation and agglomeration prior to use. Lime stabilization is widely recognized for its effectiveness in modifying soil plasticity, improving workability, and enhancing long-term strength by promoting pozzolanic reactions between lime and clay minerals[45]. The lime employed in this study had a certified purity of ≥ 90%, meeting the specifications outlined in ASTM C977-18[47] for lime used in soil stabilization. High-purity lime ensures consistent reactivity, which is crucial for reproducible test outcomes and reliable field-performance predictions. Proper storage and handling are critical for maintaining its chemical integrity, as carbonation or moisture absorption can reduce the reactivity of lime and compromise the efficiency of stabilization processes[44,45]. The selection and management of lime reflect standard geotechnical practices, ensuring compatibility with widely accepted design methodologies and laboratory protocols. Equations 1 and 2 represent the chemical reactions that constitute the hydrated lime.

$$\mathrm{Ca\ (OH)_2 + SiO_2 \rightarrow C - S - H\ \ (Calcium\ Silicate\ Hydrate)} \quad (1)$$

$$\mathrm{Ca\ (OH)_2 + Al_2O_3 \rightarrow C - A - H\ \ (Calcium\ Aluminate\ Hydrate)} \quad (2)$$

Geogrid

A uniaxial polypropylene (BP) geogrid with an aperture size of 30 × 30 mm and a tensile strength of 20 kN/m, conforming to ASTM D6637[48], was employed in this study. uniaxial geogrids are widely utilized in pavement and foundation applications because of their high tensile stiffness in both principal directions, which enables an effective load distribution and soil confinement[49]. The selected aperture size was appropriate for lateritic soils, which exhibited particle gradations conducive to interlocking and mechanical restraint when paired with a uniaxial reinforcement. The geogrid was fabricated from polypropylene, a semicrystalline thermoplastic polymer composed of repeating propylene monomer units $(C_3H_6)_n$. Its chemical structure is shown in Eq. 3.

$$\text{Polypropylene}: [-CH_2 - CH(CH_3) -]_n \quad (3)$$

This chemical configuration provides excellent resistance to biological degradation, chemical attack, and ultraviolet (UV) exposure, making polypropylene geogrids well-suited for tropical and chemically aggressive environments. The geogrid specimens were cut into circular discs with a diameter of 150 mm to fit the standard compaction molds and ensure reinforcement, uniformity, and repeatability. The integration of geogrid reinforcement aims to enhance the mechanical performance of lime stabilized lateritic soils by improving stiffness, reducing deformation, and increasing load-bearing capacity[11]. The selection and preparation processes complied with the established industry standards to ensure field relevance and experimental reproducibility in Fig. 3.

Sample formulation

The control samples consisted of untreated lateritic soil compacted with natural moisture content. Lime was incorporated at 2, 4, 6, and 8% of the dry weight of soil. The mixtures were blended with distilled water to achieve optimum moisture content (OMC). For the reinforcement studies, geogrid layers were embedded at the mid-depth and one-third depth of the compacted specimens (150 mm diameter × 150 mm height) to assess the effect of the reinforcement position. Single- and double-layered geogrid-reinforced specimens are prepared. Figure 4 showing the testing procedures for the Lateritic sample with lime at various percentange and geogrid material.

Compaction strength tests (standard proctor test)

The Standard Proctor compaction test was performed to establish the optimum moisture content (OMC) and maximum dry density (MDD) of untreated and lime stabilized lateritic soils, in accordance with ASTM D698[50]. Compaction was carried out using a 944 cm^3 cylindrical mold and a 2.5 kg rammer dropped from a height of 305 mm. The soil was compacted in three layers, with 25 blows per layer, to ensure consistent energy application. Prior to testing, the mold and its base plate were weighed to the nearest 1 g and fitted with an extension collar. Moist soil was placed into the mold in increments, and each layer slightly exceeded one-third of the mold height. After compacting each layer, the collar was removed, excess soil was trimmed flush with a straightedge, and any displaced material was replaced and pressed to preserve volume consistency. The compacted specimen, which was still in the mold, was weighed, extruded, and oven-dried at 105 ± 5°C to determine the moisture content. This procedure was repeated for multiple moisture contents to generate compaction curves, from which the OMC and MDD values were determined.

California bearing ratio (CBR)

The CBR tests were conducted under both soaked and unsoaked conditions. In the soaked condition, the samples were submerged in water for 96 h to simulate prolonged rainfall, whereas the unsoaked samples were tested immediately after the compaction. Penetration resistance was measured at depths of 2.5 mm and 5.0 mm. The setup consisted of a loading machine, plunger (50 mm diameter cylindrical rod), ring for load measurement, dial gauge for penetration measurement, and mold to contain the soil specimen. A water bath was used to soak the specimens under the soaking conditions ASTM D1883[51]. Specimen preparation and test procedure: Soil specimens were compacted to the desired density. Optimum moisture content (OMC) was determined using compaction tests. Each mold was filled with five layers and each layer was compacted to the required density. The proving ring and dial gauge were attached to the plunger. A load was applied to the plunger at the penetration rate of 1.25 mm/min. The corresponding loads were recorded at 2.5 mm and 5.0 mm. The CBR values were computed from the recorded loads.

Unconfined compressive strength (UCS) testing

Cylindrical specimens (38 mm diameter × 76 mm height) were tested using a hydraulic press at a strain/penetration rate of 1.0 mm/min. Sample collection and preparation: Lateritic soil samples were collected to ensure representativeness and to avoid contamination. The samples were air-dried and sieved to remove the coarse particles. Each test specimen was prepared by adding water to achieve the desired moisture content, compacting it into a cylindrical mold, and ensuring proper alignment in an unconfined compression apparatus ASTM D2166[52]. The specimens were mounted and the load was applied at a constant rate until failure. The maximum load at failure was recorded.

Particle size distribution

Sieve analysis was conducted to determine the particle size distribution (PSD) and assess the grading characteristics of the lateritic soil in accordance with ASTM D422-63. Representative soil samples were oven-dried at 100 ± 5 °C for three hours and cooled to room temperature before testing. A nest of standard sieves with apertures of 2.36 mm, 1.18 mm, 0.600, 0.425, 0.300, 0.212, 0.150, and 0.075 mm was arranged in descending order, with a pan placed at the base to collect fines. The prepared soil sample was introduced into the top sieve and the stack was manually agitated for 15 min to ensure adequate separation of the particles. The material retained on each sieve and in the pan was weighed, and the percentage passing through each sieve was calculated.

Atterberg limits

Atterberg limit tests, including liquid limit (LL), plastic limit (PL), and plasticity index (PI), were performed in accordance with ASTM D4318-17[53]. The liquid limit was determined using the Casagrande apparatus, with the water content corresponding to 25 blows taken as the LL. The plastic limit was obtained using the thread-rolling method, in which the soil threads were rolled by hand until crumbling occurred at a diameter of 3 mm. The plasticity index is an indicator of the soil consistency and plasticity characteristics.

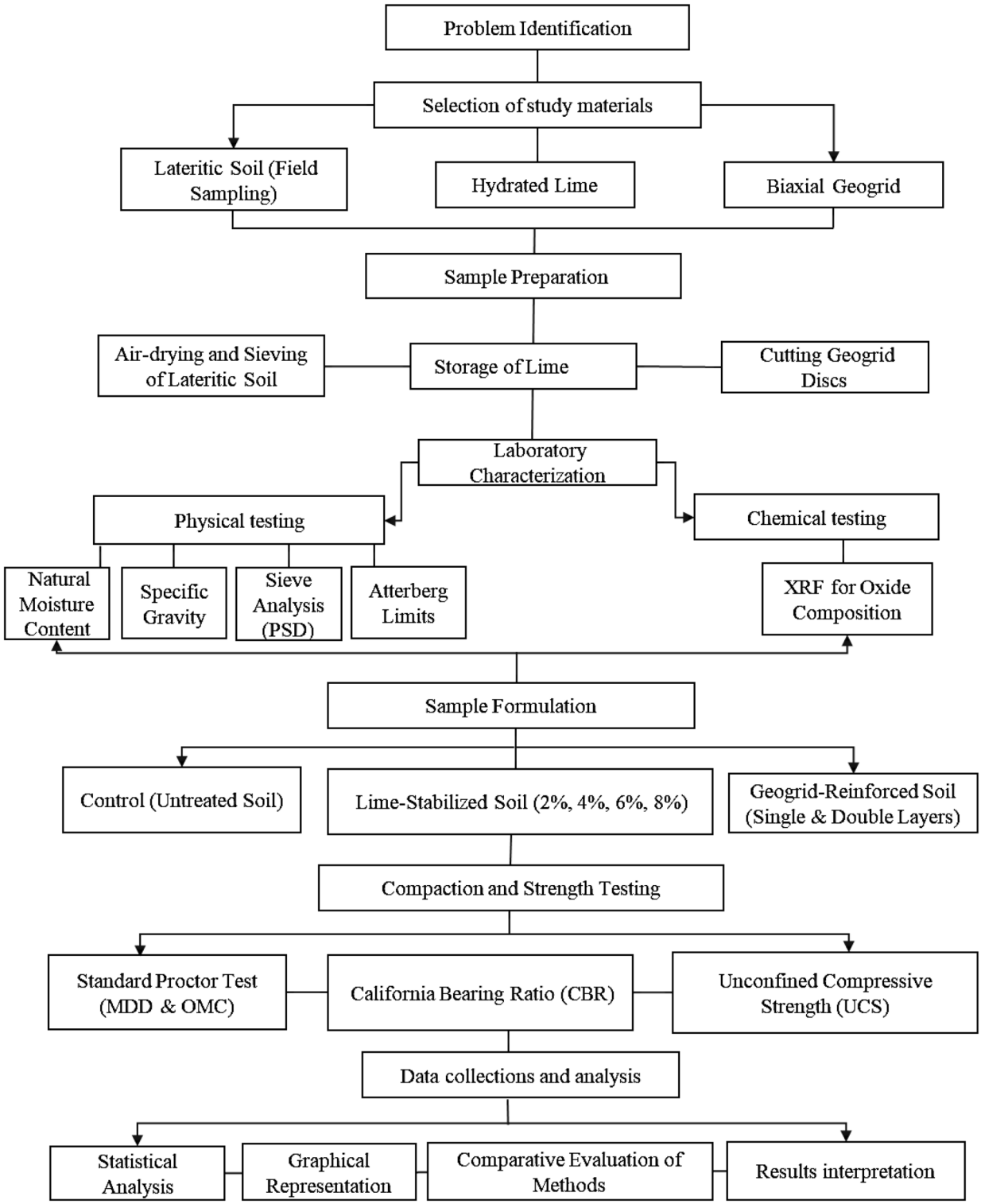

Fig. 3. Flow chart illustrating the research process.

Results and discussion

Chemical and mineralogical composition

Mineral quantification using Rietveld refinement confirmed the relative abundances of quartz (32%), kaolinite (25%), and goethite (8%). These results align with the tropical laterite mineralogy, which is dominated by low-activity clay minerals. The diffractograms and peak assignments were included for transparency. Qualitative and quantitative X-ray diffraction (XRD) analyses revealed five dominant mineral phases in lateritic soil (Table 2). These include quartz, orthoclase, lime, albite, and goethite, which contribute to the geochemical behavior of

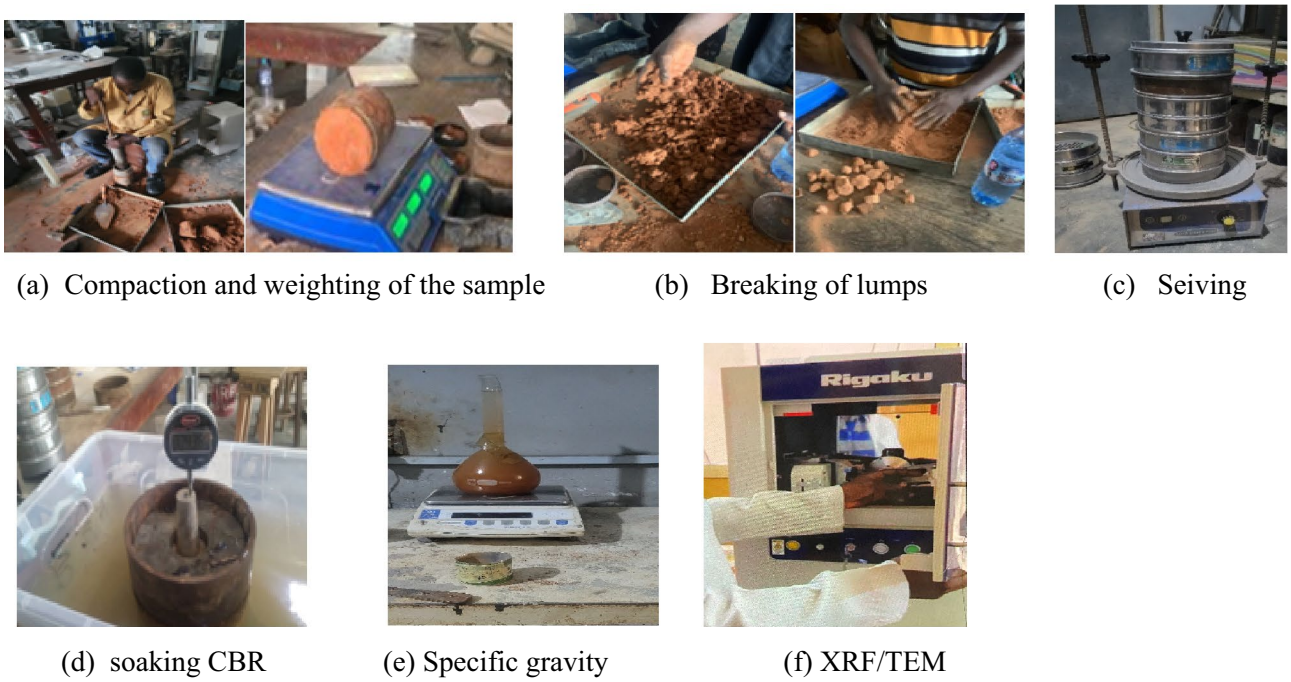

(a) Compaction and weighting of the sample (b) Breaking of lumps (c) Seiving

(d) soaking CBR (e) Specific gravity (f) XRF/TEM

Fig. 4. Testing procedures for the Lateritic sample with lime at various percentange and geogrid material.

Mineral phase	Chemical formula	Primary component	Likely source
Quartz	SiO_2	Silica	Laterite
Orthoclase	Al_2O_3 K_2O_6 SiO_2	Alumino-silicates	Laterite (clay mineral)
Lime	CaO	Calcium Oxide	Stabilizer
Albite	Na Al Si_3O_8	Feldspar (Sodium)	Laterite
Goethite	$Fe_2O_3{\cdot}H_2O$	Iron Oxide	Laterite

Table 2. Identified mineral phases in lateritic soil.

Oxide	Lateritic soil (%)	Hydrated lime (%)
SiO_2	51	3.12
Al_2O_3 (Alumina)	45	1.20
Fe_2O_3 (iron oxide)	0.9	0.87
CaO (calcium oxide)	1.5	84.62
Sodium ($NaAlSi_3O_8$)	2.1	6.21
Others	–	4.00

Table 3. Chemical composition of lateritic soil and hydrated lime.

the soil. The oxide composition determined by X-ray fluorescence (XRF) showed SiO_2 = 52.4%, Al_2O_3 = 25.1%, Fe_2O_3 = 5.2%, CaO = 2.4%, and MgO = 1.6%, consistent with siliceous–aluminous lateritic soils of low natural reactivity. X-ray diffraction (XRD) analysis identified the dominant minerals as kaolinite, quartz, gibbsite, and goethite, with minor peaks for orthoclase and albite.

Chemical composition reflects that the lateritic soil was predominantly composed of silica (51%) and alumina (45%), with minor contributions from iron oxide (0.9%) and calcium oxide (1.5%) (Table 3). This chemical profile reflects the typical mineralogy of tropical lateritic soils, which are dominated by quartz, aluminosilicate clays (orthoclase and albite) and iron oxides (goethite). The low native calcium content indicates that the soil is inherently non-calcareous with limited natural cementation potential. The hydrated lime sample exhibited an exceptionally high CaO content (84.62%), accompanied by trace amounts of silica, alumina, and sodium oxide. This composition confirms the suitability of lime as a chemical stabilizer, as the high calcium oxide concentration readily hydrates to form calcium hydroxide ($Ca(OH)_2$), initiating pozzolanic reactions with the

silica and alumina present in the soil. Cation exchange, flocculation, and pozzolanic reactions occur when lime is introduced into silica- and alumina-rich soil.

Immediate Reactions (Short-Term Effects) The exchange of calcium ions with adsorbed cations (Na^+ and K^+) on clay particle surfaces reduces the double-layer thickness, thereby promoting flocculation and particle aggregation. This leads to immediate improvements in soil workability and reduced plasticity, as reflected in the Atterberg limit results.

Pozzolanic Reactions (Long-Term Effects) Over time, the high CaO content of lime reacts with the available silica and alumina to form cementitious calcium silicate hydrates (C-S-H) and calcium aluminate hydrates (C-A-H). These compounds enhanced strength and stiffness and improved the load-bearing capacity of the soil, as confirmed by the CBR and UCS test results.

pH Rise and Dissolution of Silica/Alumina The introduction of lime increases the pH of the soil above 12.4, promoting the dissolution of amorphous silica and alumina from clay minerals and accelerating the pozzolanic reaction process. The relatively high silica-to-alumina ratio observed in the soil suggests a favorable reactivity profile, where lime addition is expected to yield substantial improvements in mechanical properties. The significant difference in CaO content between the untreated soil (1.5%) and lime (84.62%) underscores the role of lime in chemically transforming the soil structure and strength characteristics. These findings provide a strong geochemical basis for the observed experimental improvements in compaction characteristics, CBR values, and UCS results with lime stabilization, particularly at 4–6% lime content, which is often considered optimal for lateritic soils.

Effect of moisture content on shear strength

Moisture content governs the shear strength of fine-grained lateritic soils through three coupled mechanisms: (1) changes in the soil fabric and effective stress with degree of saturation S_r, (2) evolution of suction along the soil–water characteristic curve (SWCC), and (3) binder- and reinforcement-dependent interactions (lime hydration/pozzolanicity; geogrid confinement). For compacted laterites, strength typically peaks near the Optimum Moisture Content (OMC) and declines for both drier-than-optimum and wetter-than-optimum states.

Mechanistic framework

For unsaturated states, the extended effective stress can be expressed with Bishop's parameter $\chi\,(S_r)$ in Eq. (4):

$$\sigma' = \sigma - u_a + \chi\,(S_r)\ (u_a - u_w) \tag{4}$$

where u_a and u_w are pore-air and pore-water pressures. As moisture increases (at constant net stress $\sigma - u_a$), matric suction $(u_a - u_w)$ decreases, reducing σ' and, via Mohr–Coulomb, the mobilized shear strength as shown in Eq. (5):

$$\tau_f = c' + \sigma' \tan\varphi' \tag{5}$$

Consequently, both UCS and CBR decline as the soil moves from the dry side of optimum toward saturation. On the dry side, insufficient lubrication and incomplete kneading lead to an open, interaggregate fabric and reduced contact area; on the wet side, suction loss and pore-pressure build-up dominate (Fig. 5).

Trends observed in this study

- Untreated laterite: Standard Proctor testing gave OMC = 15.7% and MDD = 1.76 g/cm³. UCS and soaked CBR were lowest when specimens were compacted several percent wetter than OMC due to suction loss; strengths improved markedly when compacted at or just below OMC, consistent with the densest fabric and higher σ'.
- Lime-treated soil: Lime shifted the compaction curve (OMC ↑, MDD ↓), so the moisture window for peak strength also shifted. At 4–6% lime, specimens compacted within ± 1% of the new OMC achieved the highest UCS (up to 0.95 MPa at 28 days) and soaked CBR (57%). Two effects explain this: (i) adequate water is required for hydration and early cation-exchange/flocculation; (ii) excess water beyond the shifted OMC reduces suction and introduces larger, poorly drained pores before pozzolanic gels mature.
- Geogrid-reinforced mixes: Geogrid primarily affects stiffness and confinement, not intrinsic suction. Its benefit is greatest when specimens are compacted near the OMC of the host matrix; at wetter-than-optimum states, the grid still redistributes load but cannot fully compensate for suction loss.
- Combined lime + geogrid: Near the shifted OMC, chemical bonding (C–S–H/C–A–H) plus mechanical confinement produced the highest strengths (UCS >1.0 MPa; soaked CBR >65%). Moving wetter than optimum diminished gains for the same suction-related reasons, although the rate of loss was smaller than for unreinforced, un-stabilized soil.

Simple design relationships (useful for quality control)

Within a practical range around the relevant OMC, UCS and CBR can be captured with compact, field-friendly forms:

- Parabolic UCS peak around OMC (good over ± 3% moisture range) represented in Eq. (6):

$$\mathrm{UCS}\,(w) = \mathrm{UCS}_{\max}\left[1 - b\,\left(w - \mathrm{OMC}\right)^2\right], b > 0 \tag{6}$$

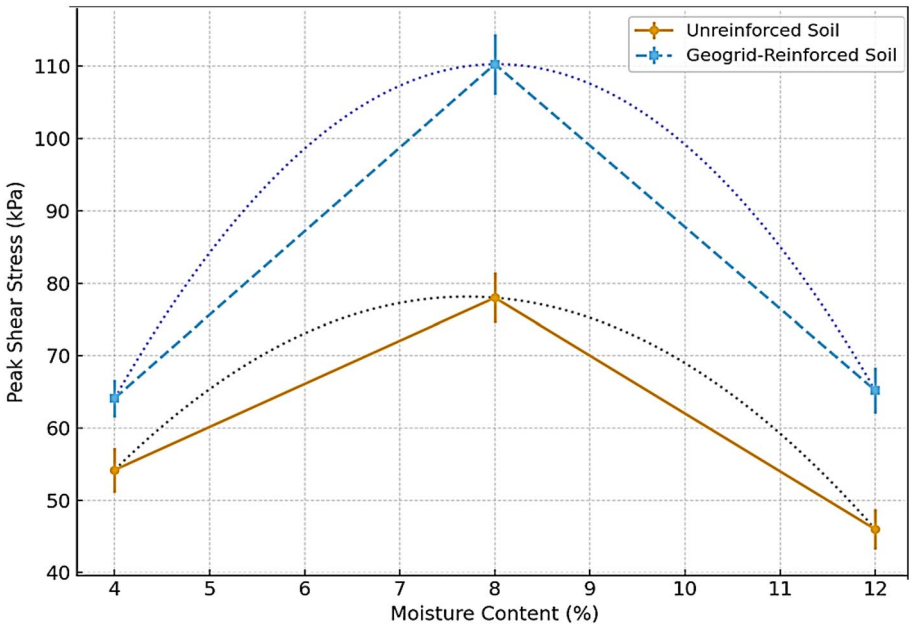

Fig. 5. Effect of moisture content on shear strength.

Parameter	Symbol	Value (mm)	Interpretation
Effective size	D_{10}	0.012	Represents 10% finer; controls permeability
Intermediate size	D_{30}	0.045	30% finer by weight
Characteristic size	D_{60}	0.155	60% finer by weight
Coefficient of uniformity	$C_u = D_{60}/D_{10}$	12.9	Indicates well-graded fines with some spread
Coefficient of curvature	$Cc = (D_{30})^2 / (D_{60} \cdot D_{10})$	1.1	Within 1–3 range, showing smooth gradation curve

Table 4. Particle-size statistics of lateritic soil.

- Approximately linear CBR loss on the wet side of OMC in Eq. (7):

$$\mathrm{CBR}\,(w) = \mathrm{CBR}_{\mathrm{OMC}} - k\,(w - \mathrm{OMC})\,, w \geqslant \mathrm{OMC}. \tag{7}$$

Here k is project-specific (often a few CBR-points per 1% moisture for lateritic fines; larger sensitivity without lime, lower with lime + geogrid).

Practical implications for construction control

- Compact at or just below the correct OMC for the selected mix (untreated vs. lime-treated), not the untreated soil's OMC.
- Moisture tolerance bands: target OMC ± 1% for lime-treated layers to balance hydration and suction; outside ± 2% expect noticeable losses in UCS/CBR.
- Curing moisture: for lime mixes, maintain moisture during the first 7–14 days to support pozzolanic gain without creating saturation; sealed curing or light misting under covers is effective.
- Field testing: pair in-situ moisture/density (sand cone/nuclear gauge) with rapid index tests to verify the mix is near its shifted OMC; adjust water or rolling passes accordingly.
- Geogrid placement: ensure proper confinement (embedment at ~ 0.25 H for single layer; correct seating) to realize benefits when the host matrix is at the right moisture state.

In summary, moisture content controls shear strength through its impact on suction, fabric, and (for stabilized soils) reaction progress. Peak performance occurs at the OMC appropriate to the mix; lime shifts that optimum to higher water contents, while geogrid amplifies the benefit when compaction hits that moisture window.

Particle size distribution (PSD) and gradation characteristics

Particle size distribution (PSD) defines the textural composition and classification of the soil and was determined in accordance with ASTM D7928[54]. The procedure involved dry sieve analysis for coarse and intermediate fractions (4.75–0.075 mm) using a nested stack of sieves with apertures of 2.36, 1.18, 0.600, 0.425, 0.300, 0.212,

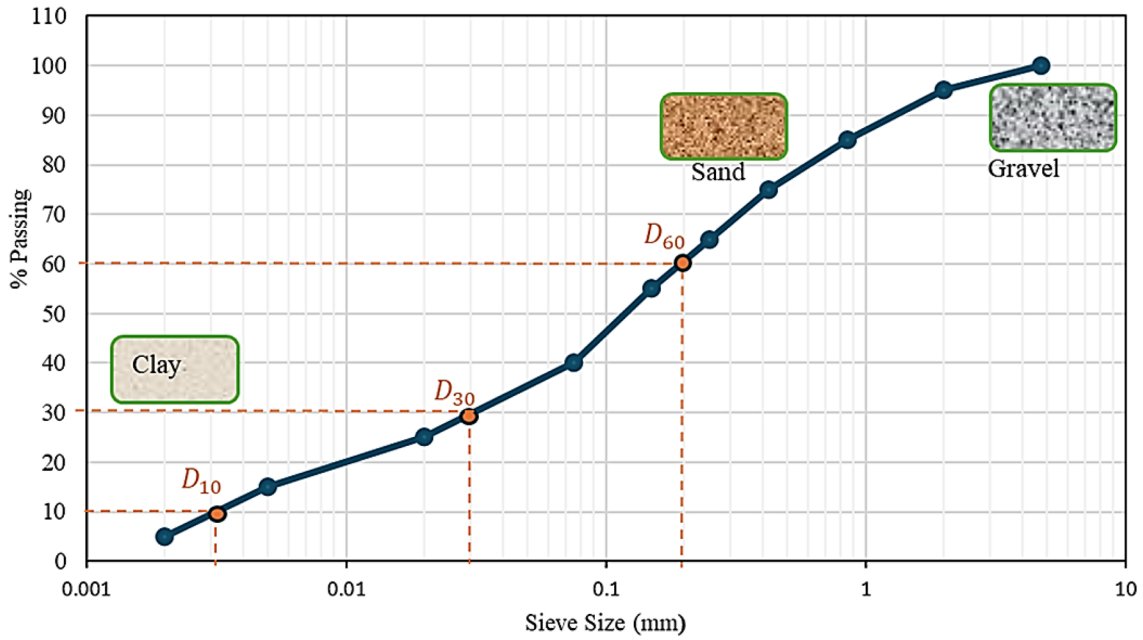

Fig. 6. Particle size distribution curve of the laterite.

Lime content (%)	Specific gravity sample
0	2.66
2	2.65
4	2.64
6	2.64
8	2.63

Table 5. Specific gravity result.

0.150, and 0.075 mm, followed by hydrometer analysis to quantify the silt and clay fractions (< 0.075 mm). Hydrometer readings were corrected for temperature and meniscus effects to ensure accuracy for fine particles (< 0.002 mm). Figure 6 presents the complete particle-size distribution curve of the lateritic soil, showing a predominance of fine particles with limited coarse content. The cumulative percentage passing indicates 66% fner than 0.075 mm, confirming the soil's fine-grained nature. Characteristic diameters obtained from the curve are summarized in Table 4.

Effects on specific gravity of lateritic soil with varying lime content

The specific gravity (G_s) of soil solids reflects the mineralogical composition and density of the soil matrix and serves as an indicator of changes in solid-phase chemistry during stabilization. Variations in G_s with lime content therefore provide indirect evidence of mineral replacement, hydration, and pozzolanic reactions occurring within the treated lateritic soil. The measured G_s values decreased marginally from 2.66 ± 0.02 for the untreated soil to 2.63 ± 0.01 at 8 wt% lime addition (Table 5). Statistical analysis using one-way ANOVA indicated that this reduction, although small in magnitude (1.1%), was significant at $p = 0.041$ ($\alpha = 0.05$). Each value represents the mean of three independent measurements performed according to ASTM D854-23. The observed decrease in G_s is attributed to three concurrent mechanisms:

- Substitution by lower-density lime compounds: The replacement of heavier silicate and ferric minerals (quartz, goethite; $G_s = 2.65$-2.75) with lower-density calcium hydroxide ($G_s = 2.34$) decreases the mean density of soil solids.
- Formation of hydration and pozzolanic products: X-ray diffraction and electron microscopy confirm the generation of amorphous calcium silicate hydrate (C–S–H) and calcium aluminate hydrate (C–A–H) gels. These products are less dense and more porous than the parent minerals, further lowering G_s.
- Flocculation and aggregation effects: Cation exchange between Ca^{2+} and monovalent cations (Na^+, K^+) causes clay platelet flocculation and the development of micro-voids within aggregates, which reduces the apparent density of the solid phase.

Despite the minor reduction in G_s, lime treatment markedly enhanced mechanical performance. The correlation between G_s and unconfined compressive strength (UCS) showed an inverse trend ($R^2 = 0.87$): as G_s decreased slightly, UCS increased from 300 ± 15 kPa (untreated) to 950 ± 40 kPa at 6 wt% lime. This relationship suggests that microstructural reorganization and cementitious bonding dominate the strength behavior, while the reduction in density is a secondary effect of the chemical transformation. The small but consistent decline in specific gravity therefore signifies successful pozzolanic alteration rather than material degradation. Similar magnitudes of change (1–2%) have been reported for lime-stabilized lateritic soils in tropical environments, confirming the reproducibility of this trend.

Atterberg limits of lime-stabilized lateritic soil

The Atterberg limits of the lateritic soil samples exhibited distinct and systematic variation with increasing lime content. The liquid limit (LL) decreased progressively from 45% at 0% lime to 33% at 8% lime, whereas the plastic limit (PL) increased from 15 to 27%. Consequently, the plasticity index (PI) dropped sharply from 30% to 6%, demonstrating a significant reduction in the plasticity of the soil. These changes reflect the profound influence of lime on the physicochemical behavior of clay-rich lateritic soils. The observed decrease in LL can be attributed to the lime-induced cation exchange and flocculation of clay particles. The introduction of calcium ions (Ca^{2+}) from hydrated lime replaces exchangeable cations on the clay surface, neutralizing negative charges and reducing the thickness of the diffuse double layer. This process causes clay particles to aggregate into larger and more stable clusters, thereby reducing the capacity of soil to retain water in the liquid state. Conversely, an increase in the PL was indicative of an enhanced soil structure and improved workability. Lime treatment reduces clay activity, leading to a stiffer soil matrix that requires higher moisture content to reach plastic consistency. The simultaneous reduction in the PI reflects a shift from highly plastic soil to a material of low to medium plasticity, which significantly lowers the susceptibility of the soil to volume changes during wetting and drying cycles.

From an engineering perspective, these results are consistent with those of previous studies on lime stabilization in tropical and lateritic soils, where lime addition is known to decrease plasticity, improve compaction characteristics, and increase long-term strength. The data suggest that a lime content of 6–8% by weight is effective in achieving substantial stabilization of this lateritic soil, making it more suitable for road subgrade, embankment, and foundation applications. The stabilization process is further enhanced by pozzolanic reactions between lime and silica/alumina in the soil, leading to the formation of calcium silicate hydrates (C-S-H) and calcium aluminate hydrates (C-A-H), which impart additional binding and strength over time. Overall, the Atterberg limit analysis confirmed that lime stabilization is a robust technique for modifying the properties of fine-grained lateritic soils, offering improvements in workability, volume stability, and performance underload.

Compaction characteristics of lime-stabilized lateritic soil

The compaction test results (Fig. 7) show a clear trend of decreasing Maximum Dry Density (MDD) and increasing Optimum Moisture Content (OMC) with progressive lime addition. The untreated lateritic soil exhibits an MDD of 1.76 g/cm³ and an OMC of 15.7%. As the lime content increased to 8%, MDD decreases to 1.60 g/cm³, while OMC increases to 18.9%.

This behavior is typical of fine-grained soils stabilized with lime and can be attributed to several key mechanisms.

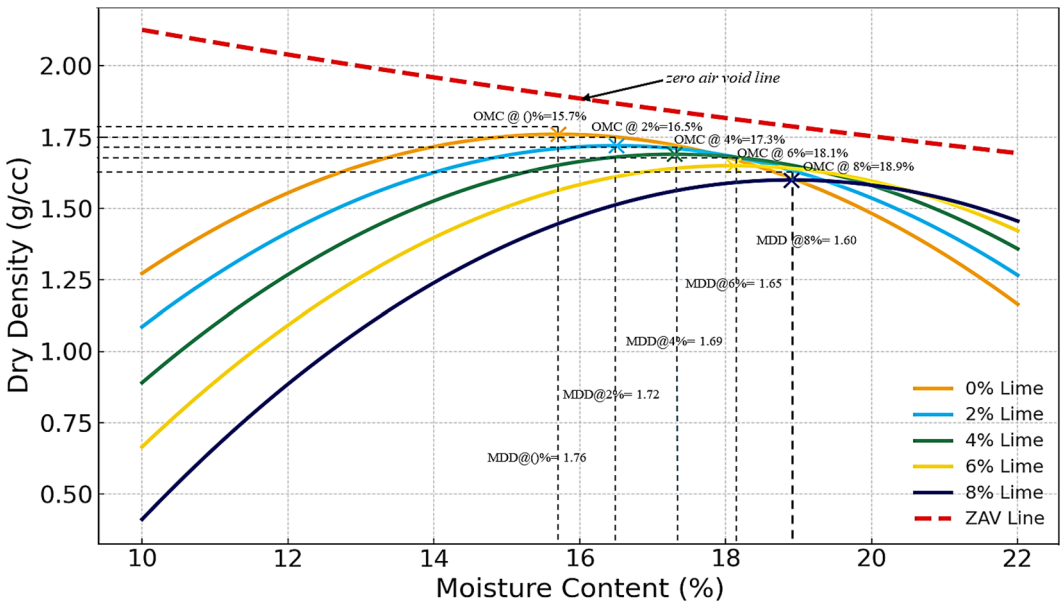

Fig. 7. Trend showing decreasing maximum dry density (MDD) and increasing optimum moisture content (OMC) with progressive lime addition.

1. Lime particles have a lower specific gravity (~2.2–2.4) than the dominant mineral constituents of lateritic soils (quartz, alumina, and iron oxides). Substituting heavier soil particles with lighter lime particles reduces the overall mass per unit volume, thereby lowering the achievable dry density.
2. The addition of lime induces cation exchange between calcium ions (Ca^{2+}) and exchangeable cations in the clay mineral lattice. This process neutralizes negative changes on clay surfaces, leading to flocculation and the formation of a more open aggregated soil structure. Such a structure is less capable of achieving high density during compaction.
3. The increase in OMC is linked to the additional water required for lime hydration and pozzolanic reactions. The reaction of lime with silica and alumina in the soil forms calcium silicate hydrates (C-S-H) and calcium aluminate hydrates (C-A-H), which consume water, thus shifting the moisture-density relationship toward higher water contents.
4. While the dry density decreased slightly, lime treatment enhanced soil stiffness, reduced plasticity, and improved long-term strength. This aligns with stabilization objectives, where chemical modification of the soil matrix is more critical than achieving high densities alone. A higher OMC facilitates easier compaction in the field, contributing to more consistent layer placement and density control.

The results emphasize that lime stabilized lateritic soils should be compacted at higher moisture contents than untreated soils, following the shifted compaction curve. A lower MDD does not signify a loss in performance; instead, it reflects the fundamental transformation of the soil structure and mineralogy owing to lime treatment. When combined with other stabilization techniques, such as geogrid reinforcement, this approach yields a pavement subgrade material that is more durable, less moisture-sensitive, and capable of supporting higher traffic loads in tropical climates.

Effect of geogrid reinforcement on CBR of lime-stabilized lateritic soil

The inclusion of a uniaxial polypropylene geogrid (tensile strength = 22 kN/m; aperture = 30 mm) significantly improved the load-bearing behavior. Tests were performed on lime-stabilized samples (6% lime, 28-day curing) with single and double geogrid layers placed at mid-depth and one-third depth, respectively. Each condition was replicated three times, and the error bars in Fig. 8 represent ± 1 SD. The soaked CBR increased from 32 ± 1.3% (single layer) to 43 ± 1.5% (double layer) 95% gain over unreinforced soil. The ANOVA confirmed that this improvement was significant ($p < 0.01$). Interface shear testing ASTM D5321[55] yielded an interface friction angle of 36° and an adhesion of 24 kPa, validating the strong soil–geogrid interaction. These results confirm that the reinforcement provides lateral confinement, limits rutting, and enhances load distribution, which is consistent with the interlock–tension mechanism described by Kwon and Tutumluer[8]. Design guidance derived from these findings recommend placing the geogrid at approximately 0.25 H depth, with spacing ≤ 1.0B, for maximum benefit in tropical subgrades. A brief economic comparison showed a 22% costsaving relative to cement stabilization, reinforcing the practical viability of this approach.

Unconfined compressive strength

Figure 9 shows the unconfined compressive strength (UCS) values increased with lime content up to an optimum of 6%, followed by a slight decline at 8%. The untreated soil exhibited 300 ± 15 kPa, while 6% lime-treated samples achieved 950 ± 40 kPa, representing a threefold improvement. The ANOVA and Tukey's HSD tests ($p < 0.05$) confirmed the statistical significance of this optimum. Mechanistically, early strength gain (≤7 days) results from cation exchange and flocculation, while later gains (14–28 days) stem from the pozzolanic formation of C–S–H and C–A–H gels. These products were verified via XRD (Fig. 5) and SEM (Figs. 10, 11, 12),

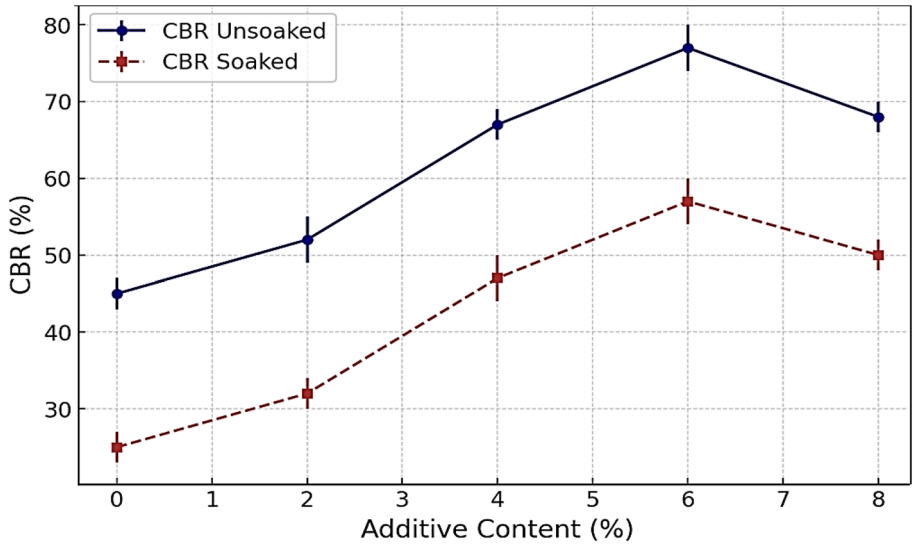

Fig. 8. CBR correlation for un-soaked and soaked for laterite with hydrated lime and geogrid.

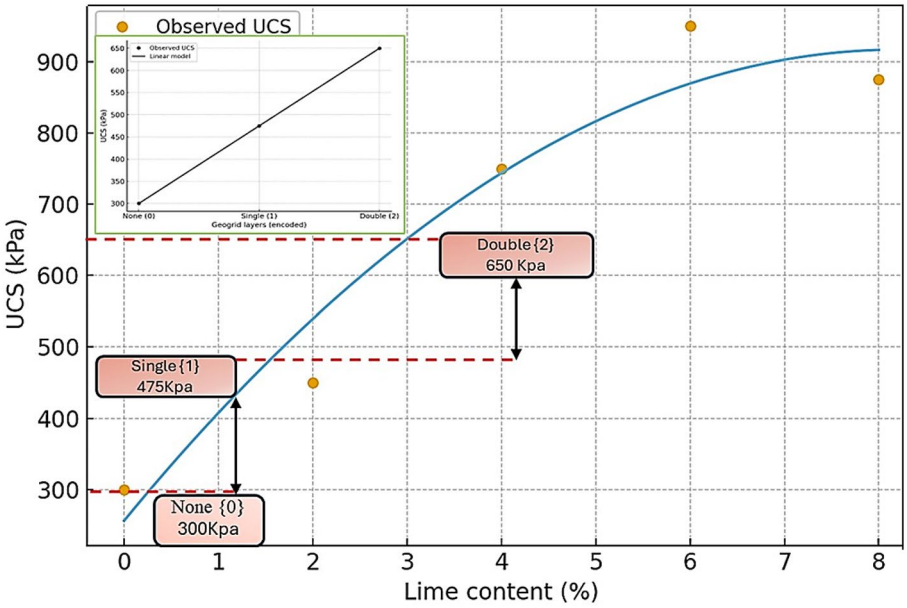

Fig. 9. Unconfined compressive strength lime-stabilized laterite with geogrid.

which showed amorphous gel phases rich in Ca and Si. Geogrid reinforcement further enhanced the UCS by ~ 20%, attributed to tension transfer and confinement at the soil–grid interface. The combined lime + geogrid system achieved > 1.0 MPa UCS after 28 days, exceeding subgrade design thresholds for heavy-traffic pavements. Nevertheless, this suitability should be interpreted cautiously, as long-term durability and field validation are still required before large-scale adoption. Tables 6 and 7 illustrate the UCS variation of lime content and geogrid layers respectively.

Microstructural and mechanistic analysis

X-ray diffraction (XRD) analysis

The XRD diffractograms of the untreated and lime-stabilized lateritic soils (Fig. 5a, b) reveal distinct mineralogical transformations induced by lime addition. The untreated soil is dominated by quartz (SiO_2), kaolinite ($Al_2Si_2O_5(OH)_4$), gibbsite ($Al(OH)_3$), and minor goethite (FeO·OH) peaks, indicating a siliceous–aluminous composition with low natural reactivity. Following 28 days of curing with 6% hydrated lime, the diffractogram exhibits attenuated kaolinite and goethite peaks alongside the emergence of broad, low-intensity humps near $2\theta = 29–32°$, characteristic of amorphous calcium silicate hydrate (C–S–H) and calcium aluminate hydrate (C–A–H) gels. These mineralogical shifts confirm that the lime reacted pozzolanically with silica and alumina from the clay minerals to produce new cementitious phases responsible for strength gain. The persistence of residual quartz and feldspar peaks implies that the reaction primarily involved the fine clay fraction rather than the coarser silty particles. The results align with the high CaO content (84.6%) of the lime measured by XRF and explain the pronounced improvement in UCS and CBR following lime treatment.

Transmission electron microscopy (TEM), energy-dispersive spectroscopy (EDS), and selected-area electron diffraction (SAED) methods

Transmission Electron Microscopy (TEM), coupled with Energy-Dispersive X-ray Spectroscopy (EDS) and Selected-Area Electron Diffraction (SAED), was employed to examine the nanoscale morphology, chemical composition, and crystallinity of the untreated and lime-stabilized lateritic soil samples, as well as hydrated lime reference material. The combined analysis provided insight into the physicochemical mechanisms governing lime–soil interactions and the formation of cementitious reaction products.

Sample preparation

Representative soil specimens were selected from the control (untreated), 6 wt% lime-stabilized, and lime + geogrid-stabilized conditions after 28 days of curing at 25 ± 2 °C and 95 ± 2% relative humidity. Samples were gently disaggregated and vacuum-impregnated with low-viscosity epoxy resin to preserve microstructural features. Thin sections were mechanically ground to a thickness of approximately 80–100 µm and then ion-milled using an argon beam (3–5 kV, ≤ 5° incidence) until electron transparency was achieved (~ 100 nm). Hydrated lime reference material was prepared by dispersing a dilute lime slurry on lacey carbon TEM grids, followed by ambient drying under a desiccator to prevent carbonation.

Instrumentation and imaging conditions

High-resolution imaging was conducted using a JEOL JEM-2100 transmission electron microscope operating at 200 kV accelerating voltage, equipped with a silicon drift detector (SDD) for EDS microanalysis and a double-

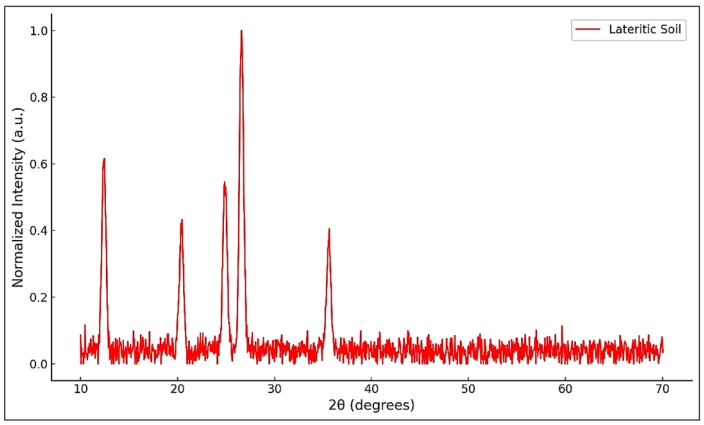

(a)

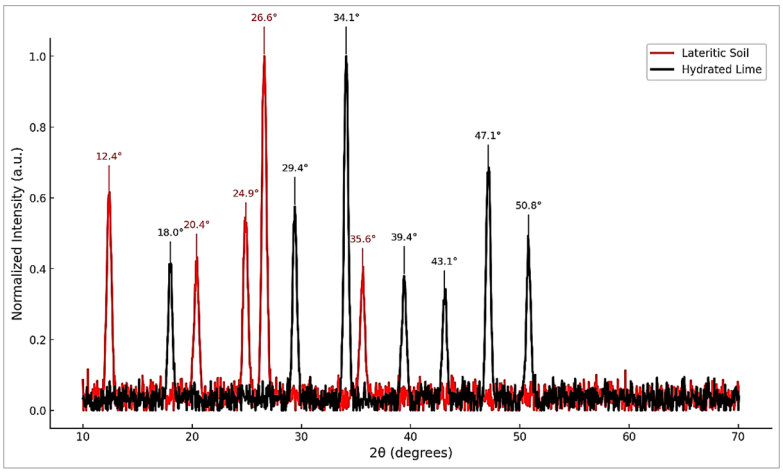

(b)

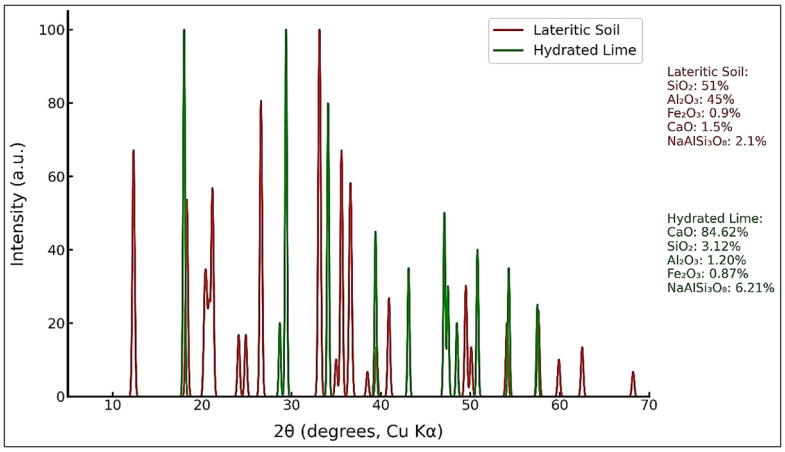

(c)

Fig. 10. X-ray diffraction analysis **a** laterite, **b** lime-stabilized laterite, **c** EDS spectra of lime and laterite.

tilt sample holder for orientation control. Bright-field (BF), dark-field (DF), and high-resolution (HRTEM) modes were employed to observe lattice structures and interparticle bonding zones. Representative fields (≥ 5 per specimen) were recorded to ensure statistical reproducibility.

EDS microanalysis

Elemental mapping and point analyses were performed using the integrated SDD detector with an energy resolution of ≤ 127 eV at Mn Kα. Quantitative data were processed with Cliff–Lorimer k-factor correction and

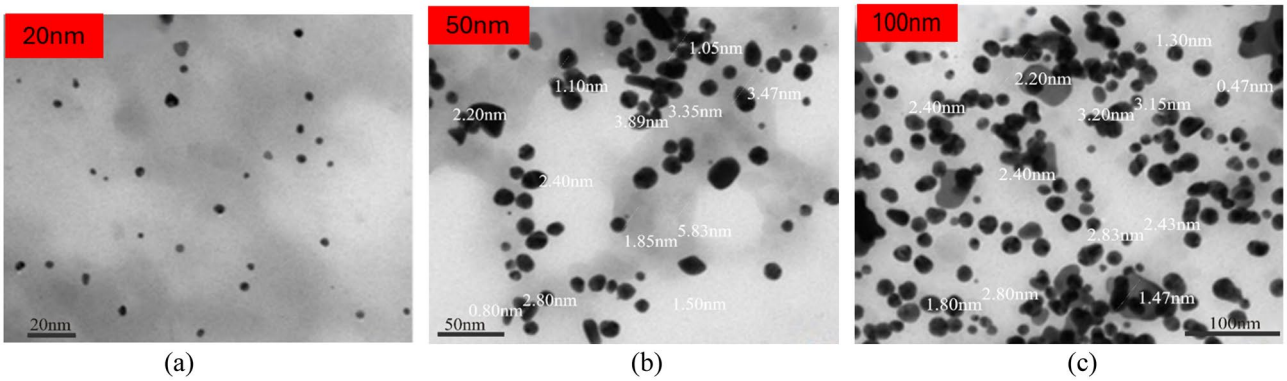

Fig. 11. **a** Untreated lateritic soil showing dispersed platelet structure and open pores; **b** lime-treated soil exhibiting flocculated aggregates and gel bridges indicative of C–S–H/C–A–H formation; **c** lime + geogrid interface showing adhesive gel films on polypropylene ribs and reduced interparticle voids.

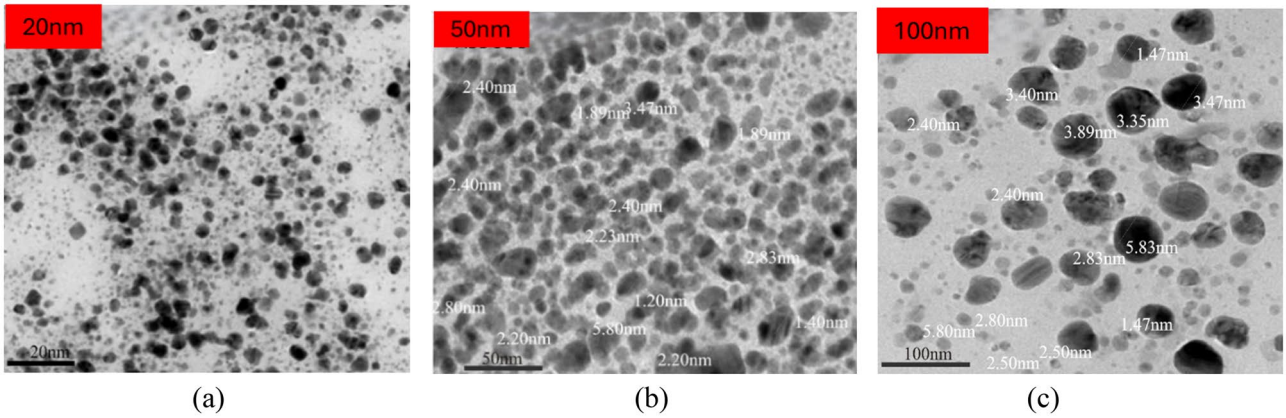

Fig. 12. Hydrated lime microstructure and reactivity. **a** TEM micrograph of hydrated lime showing hexagonal portlandite crystals (0.25–0.6 µm) within a porous matrix, scale bar = 200 nm, ×50,000, 200 kV; **b** $Ca(OH)_2$ composition and SAED pattern indexed to portlandite; **c** TEM images of lime interacting with lateritic soil particles.

Additive content (%)	Compressive strength (kpa)
0	300
2	450
4	750
6	950
8	875

Table 6. UCS variation with lime content.

Geogrid layer	UCS (kPa)
None	300
Single	475
Double	650

Table 7. UCS variation with geogrid layers.

Condition	Median feret diameter (μm)	Alignment index (AI)	Porosity (%)	Interparticle spacing (nm)	Ca/Si (molar)	Dominant phase (SAED)
Untreated (Control)	0.8 ± 0.1	0.62 ± 0.03	38 ± 2	45–80	0.02 ± 0.01	Kaolinite, Goethite
Lime-treated (6%)	1.4 ± 0.2	0.78 ± 0.04	27 ± 2	25–40	0.32 ± 0.04	Amorphous C–S–H/C–A–H
Lime + Geogrid (6%)	1.6 ± 0.2	0.81 ± 0.03	15 ± 1	15–25	0.45 ± 0.06	Amorphous + weak crystals

Table 8. Quantitative TEM metrics of lateritic soil samples.

Parameter	Mean ± SD	Units	Interpretation
Crystal diameter (D_{50})	0.37 ± 0.08	μm	Fine plate-like portlandite
Microporosity	21.8 ± 1.3	%	High reactive surface area
Phase-area fraction (portlandite)	0.78 ± 0.04	–	Dominant $Ca(OH)_2$ phase
Ca (wt %) from EDS	96.8 ± 1.2	%	Confirms high purity
Ca^{2+} concentration (leachate)	0.012 ± 0.001	mol L^{-1}	Rapid dissolution and ion release

Table 9. Quantitative TEM metrics for hydrated Lime.

normalized to oxide equivalents. Spatially resolved spectra were used to determine local Ca/Si and Ca/Al ratios in reaction zones and to differentiate primary soil minerals (Si, Al, Fe phases) from secondary lime reaction products (Ca–Si–Al gels).

SAED crystallographic analysis
SAED patterns were acquired from areas 200–500 nm in diameter to identify crystalline and amorphous phases. Diffraction ring indexing was performed using Digital Micrograph (Gatan) and cross-referenced with the JCPDS database. Diffuse halos at $2\theta \approx 29–32°$ were interpreted as signatures of amorphous calcium silicate hydrate (C–S–H) and calcium aluminate hydrate (C–A–H), confirming pozzolanic product formation. In contrast, distinct lattice reflections corresponding to quartz, kaolinite, and portlandite were observed in the untreated and hydrated lime specimens.

TEM microstructural analysis of lateritic soil, lime, and geogrid

High-resolution TEM provided nanoscale insight into the mechanisms of soil modification by lime and geogrid reinforcement. Thin foils were prepared from epoxy-impregnated soil crumbs using precision ion polishing (Ar^+, 3–5 kV, ≤ 5°). Imaging was performed at 200 kV in bright-field mode with a silicon drift detector (SDD) for energy-dispersive spectroscopy (EDS) and selected-area electron diffraction (SAED). For each condition, $n = 3$ specimens and ≥ 5 fields per specimen were analyzed to ensure reproducibility.

Untreated lateritic soil
TEM images (Fig. 10a) show loosely packed plate-like kaolinite and gibbsite crystals with minor goethite inclusions. The plates are randomly oriented (alignment index = 0.62), and the interparticle spacing (45–80 nm) corresponds to a high porosity (38%). EDS spectra exhibit dominant Si and Al peaks with minor Fe, while SAED rings confirm crystalline kaolinite and goethite. This dispersed arrangement explains the soil's high plasticity and moisture sensitivity.

Lime-treated soil
After 28 days of curing with 6% lime (Fig. 10b), the microstructure becomes aggregated and cohesive. Platelet domains coalesce (median Feret diameter ≈ 1.4 μm) with increased alignment (AI = 0.78) and reduced porosity (27%). EDS spectra display strong Ca enrichment (Ca/Si = 0.32 ± 0.04), and SAED patterns show diffuse halos indicating amorphous C–S–H/C–A–H formation. These cementitious gels bridge adjacent particles, reduce pore connectivity, and impart long-term strength and moisture stability.

Lime + geogrid reinforced soil
In the combined system (Fig. 10c), the region adjacent to the polypropylene ribs shows a dense, Ca-rich interphase with minimal voids (porosity = 15%). EDS confirms local Ca/Si = 0.45 ± 0.06, and SAED reveals amorphous halos with weak crystalline remnants. Thin gel films coat the polymer surface, demonstrating chemical adhesion between the pozzolanic products and the geogrid. This zone of interfacial bonding and mechanical confinement explains the superior UCS (> 1.0 MPa) and durability (≥ 90% strength retention after wet–dry cycles). The combined microscopy and diffraction results conclusively link microstructural transformation to macroscopic performance. The transition from a dispersed, moisture-sensitive fabric to a dense, cemented, and confined matrix explains the dramatic increases in UCS, CBR, and MR observed experimentally. These findings substantiate the study's central hypothesis that lime enhances chemical bonding while geogrid reinforcement provides mechanical confinement, and that their combination yields a durable, sustainable, and cost-effective stabilization strategy for tropical lateritic subgrades. Table 8 shows the quantitative TEM metric of lateritic soil samples.

Hydrated lime microstructure (TEM/EDS/SAED)

High-resolution Transmission Electron Microscopy (TEM) combined with Energy-Dispersive Spectroscopy (EDS) and Selected-Area Electron Diffraction (SAED) was employed to characterize the morphology and crystallography of the hydrated lime used for stabilization. Thin foils were prepared from powdered lime paste embedded in low-viscosity epoxy and ion-milled (Ar^+, 3–5 kV, ≤ 5°) to electron transparency. Imaging was performed at 200 kV accelerating voltage in bright-field mode using a silicon drift detector (SDD) for elemental analysis. Three replicate foils ($n = 3$) and five representative fields per specimen (≥ 15 total) were examined to ensure reproducibility. True magnifications ranged from ×30 000 – ×80 000, with scale bars (100–500 nm) shown in all micrographs.

Morphology and crystallography

The hydrated lime micrographs (Fig. 11a–c) exhibit well-defined hexagonal plate-like crystals with diameters between 0.25 μm and 0.6 μm (mean = 0.37 ± 0.08 μm) dispersed within a porous matrix. Quantitative image analysis (Table 9) determined a microporosity of ≈ 22% and a phase-area fraction of 0.78 for crystalline portlandite, indicating partial aggregation of fine crystallites and an interconnected pore network. These geometric parameters were extracted using ImageJ segmentation and validated by one-way ANOVA ($p < 0.05$).

Reactivity and dissolution behavior

To support the assertion that the porous microstructure facilitates rapid cation release, leachate analysis was performed by immersing 5 g of hydrated lime in 100 mL of de-ionized water for 24 h at 25 °C. The filtrate exhibited $[Ca^{2+}] = 0.012$ mol L^{-1}, pH = 12.4 ± 0.1, and an electrical conductivity of 11.8 mS cm^{-1}, confirming rapid dissolution and high cation availability for pozzolanic reactions. The observed porosity and fine crystal size enhance surface area, accelerating Ca^{2+} diffusion into the surrounding soil matrix during stabilization.

Interaction with soil and mechanistic pathway

Paired TEM micrographs (Fig. 11a–c) illustrate the progression from discrete portlandite plates to amorphous gel networks upon reaction with silica- and alumina-rich soil particles. The images show gel coatings bridging soil grains and partially obscuring the original hexagonal morphology, signifying the transformation of $Ca(OH)_2$ into calcium silicate hydrate (C–S–H) and calcium aluminate hydrate (C–A–H) phases. These features provide direct visual evidence of the mechanistic pathway responsible for long-term strength gain.

The combined TEM, EDS, SAED, and leachate analyses confirm that the hydrated lime consists of crystalline hexagonal portlandite with a fine crystal size and interconnected pore system that promotes rapid dissolution and cation release. Upon interaction with the siliceous–aluminous soil matrix, these Ca^{2+} ions form C–S–H and C–A–H gels that cement particles and improve the mechanical performance of the stabilized subgrade. The reproducibility, quantitative image analysis, and complementary chemistry together substantiate the mechanistic role of lime in the hybrid stabilization process. Figure 12 showing the hydrated lime microstructure and reactivity.

Conclusion

This study presented a mechanistic and comparative evaluation of lime stabilization and polypropylene geogrid reinforcement which applied independently and in combination for improving the strength and durability of a classified A-7-6 (CL–ML) lateritic subgrade from Ogun State, Nigeria. The experimental results showed that the addition of 4–6% hydrated lime optimally reduced the plasticity index from 30 to 6%, increased the unconfined compressive strength (UCS) from 300 kPa to 950 kPa, and improved the soaked California Bearing Ratio (CBR) from 22% to 57% after 28 days of curing. Geogrid reinforcement alone enhanced the soaked CBR to approximately 33% (single layer) and 43% (double layer) with negligible strength loss after repeated wet–dry cycles. The combined lime–geogrid system exhibited the highest performance (soaked CBR > 65%, UCS > 1.0 MPa), thereby exceeding AASHTO subgrade strength requirements. Microstructural analyses confirmed the formation of amorphous calcium silicate and aluminate hydrates (C–S–H and C–A–H) that chemically bond soil particles, while the geogrid provided additional mechanical confinement and load redistribution.

Theoretical and scientific contributions

The findings establish a dual-mechanism theoretical framework describing the coupled chemical–mechanical stabilization of lateritic soils. In this framework, lime induces physicochemical modification and pozzolanic bonding that enhances cohesion and long-term stiffness, whereas the geogrid mobilizes tensile restraint and interlocking to limit deformation and maintain structural integrity. Their interaction yields a synergistic, hybrid stabilization pathway that balances strength, ductility, and moisture durability. This model advances current understanding of multi-mechanism soil improvement and provides a mechanistic basis for designing low-carbon, resilient subgrade systems.

Contribution to new knowledge

By integrating microstructural (XRD, TEM, EDS) and mechanical data under unified experimental conditions, the study quantitatively links mineralogical transformation to macroscopic strength gain. It offers the first comprehensive comparison of lime and geogrid effects on the same lateritic soil and demonstrates that a 6% lime + double-layer geogrid configuration delivers optimal, sustainable performance. These outcomes provide empirical evidence and theoretical guidance for next-generation, environmentally responsible pavement subgrade design in tropical regions.

Limitations and prospects for future research

The investigation was confined to one lateritic soil type, laboratory compaction and curing conditions, and short-term durability evaluation. Future research should address long-term field validation under cyclic traffic loading, extended wet–dry and thermal cycles, and diverse tropical soil types. Additional studies should examine alternative low-carbon binders (e.g., fly ash, geopolymer, or agricultural ashes) within the proposed dual-mechanism framework and perform full life cycle and techno-economic assessments to quantify sustainability benefits.

Overall significance

This research contributes a reproducible mechanistic foundation and a new theoretical model for combined chemical and mechanical stabilization of lateritic subgrades. The demonstrated synergy between lime and geogrid represents a durable, cost-effective, and lower-carbon alternative to conventional cement stabilization, supporting the development of sustainable, resilient transportation infrastructure in tropical environments.

Data availability

The data underlying this article will be shared upon reasonable request by the corresponding author.

Received: 15 October 2025; Accepted: 20 November 2025
Published online: 27 November 2025

References

1. Amakye, S. Y. & Abbey, S. J. Understanding the performance of expansive subgrade materials treated with non-traditional stabilisers: a review. *Clean. Eng. Technol.* **4**, 100159 (2021).
2. Lillian, N., Ahmed, S. B., Krishnan, D. & Eze, V. H. U. Comprehensive evaluation of sub-base materials for road pavements, integrating California bearing ratio and triaxial compression tests for enhanced stability and durability: a systematic review. *Discov. Civ. Eng.* **2**, 116 (2025).
3. Shaikh, G., Mahajan, S., Shaikh, D. U. S., Wadekar, P. & M. N. & Scientific study of asphalt road surface distress and their role in the design of flexible pavements. *Int. J. Eng. Trends Technol.* **70**, 220–232 (2022).
4. Cota, J. et al. Improvement in durability and service of asphalt pavements through regionalization methods: a case study in Baja California, Mexico. *Sustainability* **14**, 5123 (2022).
5. Okeke, C. et al. Appropriate use of lime in the study of the physicochemical behaviour of stabilised lateritic soil under continuous water ingress. *Sustainability* **13**, 257 (2020).
6. Amadi, A. A. & Okeiyi, A. Use of quick and hydrated lime in stabilization of lateritic soil: comparative analysis of laboratory data. *Int. J. Geoeng.* **8**, 3 (2017).
7. Dhar, S. & Hussain, M. The strength and microstructural behavior of lime stabilized subgrade soil in road construction. *Int. J. Geotech. Eng.* **15**, 471–483 (2021).
8. Kwon, J. & Tutumluer, E. Geogrid base reinforcement with aggregate interlock and modeling of associated stiffness enhancement in mechanistic pavement analysis. *Transp. Res. Rec. J. Transp. Res. Board.* **2116**, 85–95 (2009).
9. Markiewicz, A., Koda, E. & Kawalec, J. Geosynthetics for filtration and stabilisation: a review. *Polymers (Basel)* **14**, 5492 (2022).
10. Styer, J., Tunstall, L., Landis, A. & Grenfell, J. Innovations in pavement design and engineering: a 2023 sustainability review. *Heliyon* **10**, e33602 (2024).
11. Naga, L., Chikhaoui, M., Cazzuffi, D. & Djerbal, L. Effect of installation damage on the behavior of a polypropylene geogrid in an aggressive environment. *Transp. Geotech.* **51**, 101523 (2025).
12. Phummiphan, I. et al. Stabilisation of marginal lateritic soil using high calcium fly ash-based geopolymer. *Road Mater. Pavement Des.* **17**, 877–891 (2016).
13. Ikechukwu, A. F. & Chibuzor, O. K. Improving resilient modulus and cyclic crack restriction of preloaded expansive subgrade treated with nano-geopolymer binder. *Arab. J. Geosci.* **15**, 1340 (2022).
14. Onyelowe, K. C., Ebid, A. M., Aneke, F. I. & Nwobia, L. I. Different AI predictive models for pavement subgrade stiffness and resilient deformation of geopolymer cement-treated lateritic soil with ordinary cement addition. *Int. J. Pavement Res. Technol.* **16**, 1113–1134 (2023).
15. Mohajerani, A. et al. Recycling waste rubber tyres in construction materials and associated environmental considerations: a review. *Resour. Conserv. Recycl.* **155**, 104679 (2020).
16. Ikechukwu, A. F., Hassan, M. M. & Moubarak, A. Resilient modulus and microstructure of unsaturated expansive subgrade stabilized with activated fly ash. *Int. J. Geotech. Eng.* **15**, 915–938 (2021).
17. Ikechukwu, A. F. & Mostafa, M. M. H. Assessing the coupling effects of nanosized fly ash and precompression stress towards mitigating subgrade cracks mobilised by traffic loading. *Nanatechnol. Environ. Eng.* **6**, 63 (2021).
18. Karabash, Z. & Cabalar, A. F. Effect of tire crumb and cement addition on triaxial shear behavior of sandy soils. *Geomech. Eng.* **8**, 1–15 (2015).
19. Cabalar, A. F., Ismael, I. A. & Yavuz, A. Use of zinc coated steel CNC milling waste for road pavement subgrade. *Transp. Geotech.* **23**, 100342 (2020).
20. Gołos, M. & Mazurowski, P. Pavement optimisation with aggregate base or asphalt layers stabilised with hexagonal geogrids. *IOP Conf. Ser. Mater. Sci. Eng.* **1202**, 012024 (2021).
21. Ebid, A. M., Nwobia, L. I., Onyelowe, K. C. & Aneke, F. I. Predicting nanobinder-improved unsaturated soil consistency limits using genetic programming and artificial neural networks. *Appl. Comput. Intell. Soft Comput.* 1–13 (2021).
22. Aneke, F. I., Mostafa, M. M. H. & El Kamash, W. Pre-compression and capillarity effect of treated expansive subgrade subjected to compressive and tensile loadings. *Case Stud. Constr. Mater.* **15**, e00575 (2021).
23. Ikechukwu, A. F. & Hassan, M. M. Assessing the extent of pavement deterioration caused by subgrade volumetric movement through moisture infiltration. *Int. J. Pavement Res. Technol.* **15**, 676–692 (2022).
24. Onyelowe, K. C., Eidgahee, D. R., Jahangir, H., Aneke, F. I. & Nwobia, L. I. Forecasting shear parameters, and sensitivity and error analyses of treated subgrade soil. *Transp. Infrastruct. Geotechnol.* **10**, 448–473 (2023).
25. Utkarsh & Jain, P. K. Enhancing the properties of swelling soils with lime, fly ash, and expanded polystyrene—a review. *Heliyon* **10**, e32908 (2024).
26. Almuaythir, S., Zaini, M. S. I. & Hasan, M. Shear strength, compressibility, and consolidation behaviour of expansive clay soil stabilized with lime and silica fume. *Sci. Rep.* **15**, 26185 (2025).
27. Cabalar, A. F. & Omar, R. A. Stabilizing a silt using waste limestone powder. *Bull. Eng. Geol. Environ.* **82**, 300 (2023).
28. Cabalar, A. F. & Alosman, S. O. Influence of rock powder on the behaviour of an organic soil. *Bull. Eng. Geol. Environ.* **80**, 8665–8676 (2021).

29. Al-Taie, A., Disfani, M., Evans, R., Arulrajah, A. & Horpibulsuk, S. Volumetric behavior and soil water characteristic curve of untreated and lime-stabilized reactive clay. *Int. J. Geomech.* **19**, 1–13 (2019).
30. Mohammadinia, A., Arulrajah, A., Haghighi, H. & Horpibulsuk, S. Effect of lime stabilization on the mechanical and micro-scale properties of recycled demolition materials. *Sustain. Cities Soc.* **30**, 58–65 (2017).
31. Patel, S. K. & Singh, B. A. Comparative study on shear strength and deformation behaviour of clayey and sandy soils reinforced with glass fibre. *Geotech. Geol. Eng.* **38**, 4831–4845 (2020).
32. Amare, M. D. & Tompai, Z. A. Review on Factors Affecting the Resilient Modulus of Subgrade Soils. *Acta Tech. Jaurinensis* **15**, 99–109. https://doi.org/10.14513/actatechjaur.00636 (2022).
33. Oyelami, C. A. & Van Rooy, J. L. A review of the use of lateritic soils in the construction/development of sustainable housing in africa: a geological perspective. *J. Afr. Earth Sci.* **119**, 226–237 (2016).
34. Onwo, E. S., Emeh, C. & Igwe, O. Effect of geochemical composition of lateritic soils on their geotechnical properties. *Indian Geotech. J.* **52**, 877–894 (2022).
35. Guimarães, A. C. R., Povuação, A. M., Nascimento, G., de Monteiro, C., Coelho, L. M. & S. N. & Assessing the potential of lateritic clayey soils for road infrastructure in tropical regions. *Materials* **18**, 1804 (2025).
36. Imoh, U. U., Apata, A. C., Esther, O. F. & Etuke, J. O. A comparative study of the effect of lime and cement kiln dust in the stabilization of laterite soil (2023).
37. Abdullahi, I., Umoh, U. U. & Aapta, A. C. Effect of varying moisture content on shear strength properties of soil. *Saudi J. Civ. Eng.* **6**, 256–263 (2022).
38. Apata, A. C., Abdullahi, I., Imoh, U. U. & Onimisi, P. D. Site investigation and shear strength properties of soil. *J. Eng. Res. Rep.* **24**, 1–12 (2023).
39. Dawodu, P. O., Akindele, A. & Imoh, U. U. Recycling of waste plastic for the production of road interlocking paving stone in Nigeria. *J. Eng. Res. Rep.* **23**, 296–301 (2022).
40. Apata, A. C., Etuke, J. O., Imoh, U. U. & Busari, U. B. A comparative study of the stabilization of two lateritic soils from South-western Nigeria for highway pavement using Palm Bunch Ash (PBA). *Discovery* **19**, 354–363 (2022).
41. Apata, A. C., Busari, B. U., Imoh, U. U., Upgrading of lateriticsoil & with pulverized porcelain tiles for highway construction. https://doi.org/10.26562/ijirae.2022.v0901.03 (2022).
42. Apata, A. C., Obiora, I. J. & Imoh, U. U. CBR correlation with index properties of natural soils of selected failed roads in Southeastern Nigeria (2022).
43. Apata, A. C., Obiora, I. J. & Imoh, U. U. Evaluations of distresses in pavement layers for selected locations in southeastern Nigeria. (2021).
44. Omolaiye, G. E., Oniyangi, A. K., ISSA, T. A. & Adam, S. B. Subsurface investigation for pre-foundation study utilizing integrated geophysical and geotechnical methods, UNILORIN campus. *Discov. Geosci.* **2**, 101 (2024).
45. Reading, P. & Martin, M. Geotechnical laboratory testing. In *ICE Handbook of Ground Investigation* 299–403. (Emerald Publishing Limited, 2025). https://doi.org/10.1108/978-1-83549-890-320251006
46. ASTM D421. Test method for unconfined compressive strength index of chemical-grouted soils. Preprint at (2022). https://doi.org/10.1520/D4219-22
47. ASTM C977-18. Preprint at (2024). https://doi.org/10.1520/C0977-18R24
48. ASTM D6637. Test method for determining tensile properties of geogrids by the single or multi-Rib tensile method. Preprint at (2023). https://doi.org/10.1520/D6637_D6637M-15R23
49. Al-Barqawi, M., Aqel, R., Wayne, M., Titi, H. & Elhajjar, R. Polymer geogrids: a review of Material, design and structure relationships. *Materials* **14**, 4745 (2021).
50. ASTM D698. Test methods for laboratory compaction characteristics of soil using Standard Effort (12,400 ft-lbf/ft3 (600 kN-m/m3)). Preprint at (2021). https://doi.org/10.1520/D0698-12R21
51. ASTM D1883. Test method for California Bearing Ratio (CBR) of Laboratory-Compacted Soils. Preprint at (2021). https://doi.org/10.1520/D1883-21
52. ASTM D2166. Preprint at (2024). https://doi.org/10.1520/D2166_D2166M-24
53. ASTM D4318-17. Preprint at (2017). https://doi.org/10.1520/D4318-17E01.
54. ASTM D7928. Test Method for Particle-Size Distribution (Gradation) of Fine-Grained Soils Using the Sedimentation (Hydrometer) Analysis. Preprint at (2021). https://doi.org/10.1520/D7928-21E01
55. ASTM D5321. Test Method for Determining the Shear Strength of Soil-Geosynthetic and Geosynthetic-Geosynthetic Interfaces by Direct Shear. Preprint at (2021). https://doi.org/10.1520/D5321_D5321M-21

Author contributions

U.U.I: Writing – original draft, Visualization, Software. A.C.A: Methodology, Data curation, and conceptualization. A.M.B: Writing – original draft, Visualization. M.M.R: Writing– review, editing, and supervision.

Funding

No funding was received.

Declarations

Competing interests

The authors declare no competing interests.

Additional information

Correspondence and requests for materials should be addressed to M.M.R.